

1 Monitoring the variations of evapotranspiration due to land use/cover change in a
2 semiarid shrubland

3 Tingting Gong, Huimin Lei, Dawen Yang, Yang Jiao, Hanbo Yang

4 State Key Laboratory of Hydrosience and Engineering, Department of Hydraulic
5 Engineering, Tsinghua University, Beijing, 100084, China

6 **Correspondence to:** Huimin Lei (leihm@tsinghua.edu.cn)

7

8 **Abstract**

9 Evapotranspiration (E_T) is an important process in the hydrological cycle, and
10 vegetation change is a primary factor that affects E_T . In this study, we analyzed the
11 annual and inter-annual characteristics of E_T using continuous observation data from
12 eddy covariance (EC) measurement over four years (1 July 2011 to 30 June 2015) in a
13 semiarid shrubland of Mu Us Sandy Land, China. The Normalized Difference
14 Vegetation Index (NDVI) was demonstrated as the predominant factor that influences
15 the seasonal variations in E_T . Additionally, during the land degradation and vegetation
16 rehabilitation processes, E_T and normalized E_T both increased due to the integrated
17 effects of the changes in vegetation type, topography, and soil surface characteristics.
18 This study could improve our understanding of the effects of land use/cover change on
19 E_T in the fragile ecosystem of semiarid regions and provide a scientific reference for
20 the sustainable management of regional land and water resources.

21 **Key words:** evapotranspiration; normalized difference vegetation index; land use/cover
22 change; eddy covariance; semiarid region

23 1 Introduction

24 Arid and semiarid biomes cover approximately 40% of the Earth's terrestrial surface
25 (Fernández, 2002). Previous studies have shown that more than 50% of precipitation
26 (P) is consumed by evapotranspiration (E_T) (Yang et al., 2007; Liu et al., 2002).
27 Moreover, a slight change in E_T could have significant influences on water cycle and
28 the ratio of E_T/P could increase to even 90% or more in these regions (Mo et al., 2004;
29 Glenn et al., 2007). In terms of physical processes, E_T is affected by net radiation
30 (Valipour et al., 2015), water vapor pressure deficit (Zhang et al., 2014), wind speed
31 (Falamarzi et al., 2014), and soil water stress (Allen et al., 1998). Moreover, vegetation
32 condition is also a crucial factor influencing E_T (Tian et al., 2015; Wang et al., 2011;
33 Piao et al., 2006; Mackay et al., 2007).

34 Vegetation change mainly include phenological change (temporal) and land
35 use/cover change (spatial). Phenological change reflects the response of plants to
36 climate change (vegetation greening and browning processes) (Ge et al., 2015), which
37 actively controls E_T through internal physiologies such as stomatal conductance (Percy
38 et al., 1989), as well as the number and sizes of stomata (Turrell, 1947). In general,
39 transpiration is directly proportional to stomatal conductance at the leaf scale (Leuning
40 et al., 1995). At the canopy scale, E_T is positively proportional to surface conductance,
41 which is an integration of stomatal conductance and leaf area (Ding et al., 2014). Thus,
42 as a good indicator of vegetation phenological change, many studies have found that
43 E_T is positively related to vegetation indexes such as Normalized Difference Vegetation
44 Index (NDVI) (Gu et al., 2007). Land use/cover change influences E_T by modifying

45 vegetation species with different transpiration rates, radiation transfers within canopy
46 (Martens et al., 2000; Panferov et al., 2001), topography (Lv et al., 2006), albedos (Zeng
47 et al., 2009), soil texture (Maayar and Chen, 2006), litter coverage (Wang, 1992), and
48 biological soil crusts (BSCs) (Yang et al., 2015, Fu et al., 2010; Liu, 2012; Eldridge and
49 Greene, 1994). These complex processes result in no consensus about the effects of
50 land use/cover change on E_T . For example, during the land degradation process, some
51 researchers found that warming air temperature was the main cause to make E_T increase
52 (Zeng and Yang, 2008; Li et al., 2000; Deffema and Freire, 2001). By contrast, a decline
53 in E_T was found along with deforestation process because of less transpiration (Snyman,
54 2001; Souza and Oyama, 2011) or higher albedo (Zeng et al., 2002). Moreover, no
55 changes in E_T during land degradation process were also reported (Hoshino et al., 2009).
56 Thus, there has been an important push to better understand how E_T responds to
57 vegetation change, especially to the land use/cover change.

58 Three methods were usually employed to assess the effects of vegetation change on
59 E_T : numerical models, paired comparative approaches and in situ field observations. In
60 these methods, numerical models are widely used (Twine et al., 2003; Feddema et al.,
61 2005; Kim et al., 2005; Li et al., 2009; Cornelissen et al., 2013; Mo et al., 2004).
62 However, model parameterization of vegetation condition is a big challenge, as the
63 aforementioned complex underlying mechanisms may not be completely considered in
64 the models. Therefore, the simulated effects of vegetation change on E_T are highly
65 dependent on model parameterizations, which may induce uncertainty (Cornelissen et
66 al., 2013; Li et al., 2009). Paired comparative approach is often considered the best

67 method, nonetheless, it is difficult to find two sites with similar meteorological
68 conditions but different vegetation conditions (Li et al., 2009; Lorup et al., 1998).
69 Moreover, the method of in situ field observations is widely used to investigate long-
70 term land-atmosphere exchanges. However, the land use/cover conditions at sites are
71 generally stable, and only the response of E_T to vegetation phenological changes can be
72 observed, such as the E_T variations in grassland (Zhang et al., 2005), mixed plantation
73 (cork oak, black locust and arborvitae) (Tong et al., 2014), vineyard (Li et al., 2015)
74 and grazed steppe (Chen et al., 2009; Vetter et al., 2012). Continuous field observations
75 under both land degradation and vegetation rehabilitation processes have rarely been
76 documented, especially in the semiarid shrubland.

77 The Mu Us Sandy Land is a semiarid shrubland ecosystem on the northern margin
78 of the Loess Plateau in China. The area covers only 40,000 km² (Dong and Zhang, 2001)
79 and is ecologically fragile (Yang et al., 2007). In such an ecosystem, sand dunes and
80 BSCs are commonly observed (Gao et al., 2014; Yang et al., 2015; Li and Li, 2000; Liu,
81 2012). Due to the existence of BSCs and dry sand layers (Wang et al., 2006; Feng, 1994;
82 Liu et al., 2006; Yuan et al., 2007), soil evaporation has been effectively retained,
83 therefore, the Mu Us Sandy Land contains abundant groundwater (Li and Li, 2000).
84 During the past decades, rapid land use/cover changes have occurred in this region due
85 to agricultural reclamation (Wu and Ci, 2002; Wang et al., 2009; Ostwald and Chen,
86 2006; Zhang et al., 2007), leading to dramatic changes in vegetation conditions. With
87 respect to the specific question of whether land use/cover change will lead to increases
88 in E_T or not, a continuous measurement of E_T under different land use/cover conditions

89 is required in this region. Coincidentally, two processes of land use/cover changes (land
90 degradation and vegetation rehabilitation) have occurred at the edge of the Mu Us
91 Sandy Land, providing us a unique opportunity to study the effects of land use/cover
92 change on E_T .

93 Hence, based on the four-year measurement of E_T by eddy covariance techniques,
94 this study analyzed the seasonal and inter-annual variations in E_T , and discussed the
95 possible reasons for the responses of E_T to land use/cover change. Our results were
96 expected to provide a scientific reference for the sustainable management of regional
97 land and water resources in the context of intensive agricultural reclamation.

98

99 2 Case study and data

100 2.1 Site description

101 The study was conducted at the Yulin flux site (N 38°26′; E 109°47′; 1233 m),
102 which was established in June 2011. This site is located in a landform transition zone
103 that changes from the Mu Us Sandy Land to the north Shaanxi Loess Plateau (Fig. 1).
104 This site is a semiarid area with temperate continental monsoon climate. According to
105 long-term climate data (1951-2012) from a meteorological station in Yulin (Fig. 1), the
106 annual precipitation varied from 235 mm to 685 mm, with a mean of 402 mm, and more
107 than 50% of annual precipitation fell in the monsoon season (July-September). The
108 mean annual air temperature was 8.4 °C over the past 61 years. The dominant soil type
109 is sand (98% sand) (saturated soil water content of 0.43 m³ m⁻³, field capacity of 0.16
110 m³ m⁻³, residual moisture content of 0.045 m³ m⁻³). There are widely distributed fixed
111 sand dunes and semi-fixed sand dunes around the site, and the depth of the dry sand

112 layer is 10 cm (Wang et al., 2006). The mean groundwater depth at our study site from
113 1 July 2011 to 30 June 2015 was 3.5 m.

114 [Figure 1 is to be inserted here]

115 Shortage of water is the critical limiting factor for vegetation growth in this site,
116 and drought-enduring vegetation (e.g., shrubs) is prevailed as a result of droughts
117 (Wang et al., 2002; Wu, 2006). The study site is mainly covered with mixed vegetation:
118 the native drought-enduring shrubs with low water demand (e.g., *Artemisia ordosica*
119 and *Salix psammophila*) (Fig. 2a) and the sparse grass (mainly distributed at the bottom
120 of sand dunes because of the better soil moisture condition) (Lv et al., 2006). The
121 maximum root depth of the shrubs was approximately 160 cm. Xiao et al. (2005)
122 reported that the growing season of *Artemisia ordosica* and *Salix psammophila* spanned
123 from late April to late September. Therefore, we defined the period from 1 May to 30
124 September as the vegetation growing season for data analysis in this study. On 15
125 August 2011 and 7 September 2011, we did surveys of the vegetation coverage by
126 randomly selecting seven samples around the flux tower (5 × 500 cm × 500 cm and 2
127 × 1000 cm × 1000 cm). We found that the vegetation coverage was 28.2% in August
128 and 27.9% in September.

129 [Figure 2 is to be inserted here]

130 At the end of June 2012, the land use/cover condition around the eastern portion of
131 the flux tower began to be changed by farmers (leaves and branches were cut, and the
132 sand dunes were bulldozed) (Fig. 2c), converting part of the natural vegetated land to
133 bare land, with the planning of planting potatoes in the future. As time went on, natural

134 grass gradually grew out in the area of bare land before potatoes were planted. Thus,
135 our study period (1 July 2011 to 30 June 2015) was divided into four periods according
136 to the land use/cover conditions: (a) Period I (1 July 2011 to 30 June 2012), the period
137 with the natural land use/cover condition (i.e., mixed sparsely distributed shrubs and
138 grass) (Fig. 2a and Fig. 2b); (b) Period II (1 July 2012 to 30 June 2013), the transitional
139 period when the land use/cover condition started to change (some natural vegetation
140 removed and sand dunes bulldozed); (c) Period III (1 July 2013 to 30 June 2014), the
141 period when the land use/cover condition constituted two parts: the natural vegetation
142 zone and the bare soil zone (Fig. 2c) and (d) Period IV (1 July 2014 to 30 June 2015),
143 the period when the bare soil zone gradually covered by regrowing grass (Fig. 2d).

144

145 2.2 Field measurements

146 2.2.1 Eddy covariance system measurements

147 Net exchange of water vapor between atmosphere and canopy at this site is
148 measured by the eddy covariance (EC) flux measurement, which assesses the fluxes of
149 land-atmosphere (such as water and energy) (Baldocchi et al., 2001). The data are
150 essential for the estimation of the water and energy balance (Franssen et al., 2010). At
151 our site, the EC system is installed at a height of 7.53 m above the ground surface, using
152 CSAT3 three-dimensional sonic anemometers (Campbell Scientific Inc., Logan, UT,
153 USA) for wind and temperature fluctuations measurements and a LI-7500A open-path
154 infrared gas analyzer (LI-COR, Inc., Lincoln, NE, USA) for water vapor content
155 measurement.

156 2.2.2 Other measurements

157 Net radiation (R_n) is measured by a net radiometer (CNR-4; KIPP&ZONEN, Delft,
158 the Netherlands), including four radiometers measuring the incoming and reflected
159 short-wave radiation (R_S), and incoming and outgoing long-wave radiation (R_L).
160 Sunshine duration (D_S) is measured by a sunshine recorder (CSD3; KIPP&ZONEN,
161 Delft, the Netherlands). Wind speed and direction (05103, Young Co. Traverse City,
162 MI, USA) are measured at 10 m above the ground surface. Precipitation (P , mm) is
163 recorded with a tipping bucket rain gauge (TE525MM; Campbell Scientific Inc., Logan,
164 UT, USA) installed at a height of 0.7 m above the ground surface. Air temperature (T_a)
165 and relative humidity (R_H) are measured by a temperature and relative humidity probe
166 (HMP45C; Campbell Scientific Inc., Logan, UT, USA) at a height of 2.6 m above the
167 ground surface. Soil water content (θ) is measured by Time Domain Reflectometry
168 (TDR) sensors (CS616; Campbell Scientific Inc., Logan, UT, USA), soil temperature
169 (T_s) is measured by thermocouples (109; Campbell Scientific Inc., Logan, UT, USA),
170 and soil heat flux (G) is measured by heat flux plates (HFP01SC; Campbell Scientific
171 Inc., Logan, UT, USA) at a depth of 0.03 m below the ground surface. These ground
172 variables (G , θ , T_s) are measured beneath the surface at two profiles: a plant canopy
173 profile and a bare soil profile. θ and T_s are measured at depths of 5, 10, 20, 40, 60,
174 80, 120 and 160 cm below the ground surface. Groundwater table is measured by an
175 automatic sensor (CS450-L; Campbell Scientific Inc., Logan, UT, USA), which is
176 installed in a groundwater well close to the tower.

177

178 2.3 Flux data processing

179 10 Hz 3-dimensional wind speed and water vapor concentrations that collected by

180 EC technique were processed to half-hourly latent heat flux (λE_T) using Eddypro
181 processing software (v5.2.0, LI-COR, Lincoln, NE USA). The main principle is that
182 λE_T can be expressed as $\overline{\rho_a w' q'}$ (where w' is the fluctuation of vertical wind
183 speed, q' is the fluctuation of specific humidity and ρ_a is the air density). The
184 software also applies the quality control of data, including spike removal, tilt correction,
185 time lag compensation, turbulent fluctuation blocking and spectral corrections. The
186 percentages of half-hourly λE_T values removed (including missing and rejected)
187 through the quality control procedure were 17.3% in Period I, 20.2% in Period II, 16.5%
188 in Period III, and 18.6% in Period IV. Almost all the removed λE_T values occurred
189 during the nighttime (89.1% in Period I, 91.3% in Period II, 92.6% in Period III, and
190 88.7% in Period IV). During the nighttime, the change in λE_T was small, and E_T
191 values were close to zero. Therefore, after removal of the nighttime λE_T values, the
192 errors of the gap-filled nighttime values based on the neighboring good data were small.
193 Moreover, nighttime λE_T values accounted for only a small proportion of the daily E_T .
194 Furthermore, the percentages of rejected and missing data in our study are similar to
195 those reported by other scholars, and these percentages in a range of 15%~31% (Falge
196 et al., 2001; Wever et al., 2002; Mauder et al., 2006). Therefore, the λE_T data set was
197 considered reliable after quality control procedure.

198 After quality control, missing and rejected data were gap-filled in order to create
199 continuous data sets. Three methods were applied in the gap-filling procedure: (1) linear
200 interpolation was used to fill gaps of less than 1-h by calculating an average of the
201 values before and after the data gap; (2) for gaps that larger than 1-h but smaller than 7

202 days, the mean diurnal variation (MDV) method (Falge et al. 2001) was used; (3) for
 203 gaps that larger than 7 days but smaller than 15 days in daily λE_T values, we fitted the
 204 relationship between daily λE_T and the daily available energy flux ($R_n - G$) in each
 205 period. We chose the function f with the highest coefficient of correlation (R) in each
 206 period (Yan et al., 2013), and the function was expressed as $f = a * (R_n - G)^2 + b * (R_n - G) + c$ (Period I: $a = 0.0014$, $b = 0.075$, $c = 10.69$, $R = 0.77$; Period II: $a =$
 207 0.0012 , $b = 0.056$, $c = 17.69$, $R = 0.67$; Period III: $a = 0.0014$, $b = 0.16$, $c = 13.24$, $R =$
 208 0.75 ; and Period IV: $a = 0.0015$, $b = -0.083$, $c = 25.87$, $R = 0.69$). Then, we used the
 209 fitted function f in each period to estimate the daily λE_T values of large gaps. In
 210 addition, gaps that larger than 7-days but smaller than 15 days mostly appeared in the
 211 winter, which accounted for a small proportion of annual λE_T .

212

213

214 3 Methodology

215 3.1 Footprint model

216 In order to determine the contributing source area of flux at our site, scalar flux
 217 footprint model proposed by Hsieh et al. (2000) was used. The analytic model
 218 accurately describes the relationship between the footprint, observation height, surface
 219 roughness, and atmospheric stability. The fetch F_f was calculated as follows,

$$220 \quad F_f/Z_m = D/(0.105 \times k^2) Z_m^{-1} |L|^{1-Q} Z_u^Q \quad (1)$$

221 where k is the von Karman constant (=0.40), D and Q are similarity constants (for
 222 stable conditions, $D = 0.28$ and $Q = 0.59$; for near neutral and neutral conditions, $D =$
 223 0.97 and $Q = 1$; for unstable conditions, $D = 2.44$ and $Q = 1.33$), L is the Obukhov
 224 Length, Z_m is the height of wind instrument (=10.0 m), Z_u is defined as (Hsieh et al.,

225 2000),

$$226 \quad Z_u = Z_m(\ln(Z_m/Z_0) - 1 + Z_m/Z_0) \quad (2)$$

227 where Z_0 is the height of momentum roughness (0.05 m).

228

229 3.2 Method of analyzing controlling factors on E_T

230 It is generally recognized that potential evapotranspiration (E_{TP}), vegetation
231 condition and soil water stress are the three main factors that control E_T (Lettenmaier
232 and Famiglietti, 2006; Chen et al., 2014). In order to decouple the effect of vegetation
233 change from the integrated effects of these three factors on E_T , we used a simple
234 equation which was similar to the FAO single crop coefficient method (Irrigation and
235 Drainage Paper No. 56 (FAO-56)). This equation can be expressed as follows:

$$236 \quad E_T = E_{TP} \times f_v(\text{vegetation}) \times f_s(\text{soil water}) \quad (3)$$

237 where $f_v(\text{vegetation})$ represents the effect of vegetation change on E_T and
238 $f_s(\text{soil water})$ represents the effect of soil water stress on E_T .

239 Moreover, $f_v(\text{vegetation})$ can be regarded as the normalized E_T , which eliminates the
240 effects of atmospheric and soil water stress on E_T and can be expressed by rearranging

241 Eq. 3:

$$242 \quad f_v(\text{vegetation}) = E_T/[E_{TP} \times f_s(\text{soil water})] \quad (4)$$

243 3.2.1 Potential evapotranspiration

244 E_{TP} (mm day⁻¹) was estimated by the following equation (Maidment, 1992) which
245 is a modification of the Penman equation:

$$246 \quad E_{TP} = \frac{\Delta}{\Delta + \gamma} (R_n - G) + \frac{\rho_a c_p / r_a}{\Delta + \gamma} \frac{VPD}{\lambda} \quad (5)$$

247 where the units of R_n and G are mm d^{-1} ; ρ_a is the air density ($= 3.486 \frac{P_a}{275+T_a}$, kg m^{-3} ,
 248 where P_a is the atmospheric pressure in kPa and T_a is in degrees Celsius); c_p is the
 249 specific heat of moist air ($=1.013 \text{ kJ kg}^{-1} \text{ } ^\circ\text{C}^{-1}$); Δ is the slope of the saturation vapor-
 250 pressure-temperature curve ($\text{kPa } ^\circ\text{C}^{-1}$); VPD is the difference between the mean
 251 saturation vapor pressure (e_s , kPa) and actual vapor pressure (e_a , kPa); and λ is the
 252 latent heat of vaporization of water ($=2.51 \text{ MJ kg}^{-1}$). γ is the psychrometric constant
 253 ($\text{kPa } ^\circ\text{C}^{-1}$), which is calculated by the following equation:

$$254 \quad \gamma = \frac{c_p P_a}{\varepsilon \lambda} \quad (6)$$

255 where ε is the ratio of the molecular weight of water vapor to that of dry air ($=0.622$).

256 r_a is the aerodynamic resistance, which can be calculated as follows (Penman, 1948):

$$257 \quad r_a = \frac{4.72[\ln(\frac{Z_h}{Z_{ao}})][\ln(\frac{Z_h}{Z_{ao}})]}{1+0.536U_2} \quad (7)$$

258 where Z_h is the height at which meteorological variables are measured (2 m), and Z_{ao}

259 is the aerodynamic roughness of surface (0.00137 m) (Penman, 1963); U_2 is the daily

260 wind speed at a height of 2.0 m (m s^{-1}), and it was calculated by the wind speed at the

261 height of 10.0 m (U_{10} , m s^{-1}):

$$262 \quad U_2 = U_{10} \frac{4.87}{\ln(67.8*10^{-5.42})} \quad (8)$$

263 3.2.2 Vegetation parameters

264 In this study, vegetation phenology was represented by Moderate Resolution

265 Imaging Spectroradiometer (MODIS)-NDVI data when the land use/cover conditions

266 were fixed. NDVI is sufficiently stable to reflect the seasonal changes of any vegetation

267 (Huete et.al, 2002). Higher NDVI generally reflect the greater photosynthetic capacity

268 (greenness) of vegetation canopy (Gu et al., 2007; Tucker, 1979). The daily NDVI was

269 calculated by daily surface reflectance data:

$$270 \quad NDVI = \frac{NIR-VIS}{NIR+VIS} \quad (9)$$

271 where NIR is the spectral response in the near-infrared band (857 nm) and VIS is the
272 visible red radiation band (645 nm). In this study, NDVI was calculated by using
273 MODIS/Terra data (MOD09GQ) ($NDVI_{Terra}$) and MODIS/Aqua data (MYD09GQ)
274 ($NDVI_{Aqua}$) (<http://reverb.echo.nasa.gov>), respectively. As we found that there were
275 slight differences ($|NDVI_{Terra} - NDVI_{Aqua}| = 0.01 \pm 0.0075$) between $NDVI_{Terra}$
276 and $NDVI_{Aqua}$, we calculated NDVI by averaging $NDVI_{Terra}$ and $NDVI_{Aqua}$ in
277 order to eliminate the impacts of such differences. The calculated NDVI values were
278 then filtered to remove anomalous hikes and drops (Lunetta et al., 2006), and the
279 smoothing spline method was used to produce a smoother profile.

280 Theoretically, land use/cover change can be evaluated by comparing the land
281 use/cover maps in two different periods. However, transient land use/cover maps were
282 unavailable at our site. Therefore, we separated the study area within the footprint into
283 two zones: the undisturbed zone without any land use/cover change was deemed as
284 zone A and the disturbed zone with land use/cover change was deemed as zone B. In
285 zone A, vegetation change included only vegetation phenological change; however, in
286 zone B, there were not only vegetation phenological change but also land use/cover
287 change. Based on the assumption that the phenological change caused by climate in the
288 two zones were the same, we defined an indicator (D_{lu}) as a measure of land use/cover
289 change:

$$290 \quad D_{lu} = M_A - M_B \quad (10)$$

291 where M_A and M_B are the monthly vegetation coverages of zone A and zone B,
 292 respectively. The monthly vegetation coverage was calculated by monthly NDVI values
 293 (Gutman and Ignatov, 1998):

$$294 \quad M = (\text{NDVI} - \text{NDVI}_{\min}) / (\text{NDVI}_{\max} - \text{NDVI}_{\min}) \quad (11)$$

295 where NDVI_{\max} is the maximum value (0.8 in this study) and NDVI_{\min} is the
 296 minimum value (0.05 in this study) (Gutman and Ignatov, 1998). The calculated
 297 monthly M values (27.6% and 24.2%) were consistent with the measured vegetation
 298 coverages in August 2011 (28.2%) and September 2011 (27.9%) at our study site.

299 3.2.3 Soil water stress

300 The effects of the soil water stress on E_T can be described in three stages (Idso et
 301 al., 1974), stage 1: the soil water is enough to satisfy the potential evaporation rate
 302 ($f_s=1$); stage 2: the soil is drying and water availability limits E_T ($0 < f_s < 1$); and stage 3:
 303 the soil is dry and evaporation can be considered negligible ($f_s=0$). We used daily soil
 304 water content in the root depth (θ_r) to estimate f_s by the following expression (Hu et
 305 al., 2006):

$$306 \quad f_s = \begin{cases} = 1 & \theta_r > \theta_k \\ = 0 & \theta_r < \theta_w \\ = \frac{\theta_r - \theta_w}{\theta_k - \theta_w} & \theta_w \leq \theta_r \leq \theta_k \end{cases} \quad (12)$$

307 where θ_w is the wilting value and θ_k is the stable field capacity which is considered
 308 to be equivalent to 60% of the field capacity (Lei et al., 1988; Wang et al., 2008). θ_r
 309 was calculated by measured soil water contents at different depths (θ_i , where $i = 5, 10,$
 310 $20, 40, 60, 80, 120$ and 160 cm). From land surface to the depth of 5 cm, the soil water
 311 profile was assumed triangular, while at other depths, the soil water profiles were

312 assumed trapezoidal. Therefore, the soil moisture of root zone was calculated as:

$$313 \quad \theta_r = \frac{0.5 \left[\begin{array}{l} 5\theta_5 + (\theta_5 + \theta_{10}) * (10 - 5) + (\theta_{10} + \theta_{20}) * (20 - 10) \\ + (\theta_{20} + \theta_{40}) * (40 - 20) + (\theta_{40} + \theta_{60}) * (60 - 40) \\ + (\theta_{60} + \theta_{80}) * (80 - 60) + (\theta_{80} + \theta_{120}) * (120 - 80) \\ + (\theta_{120} + \theta_{160}) * (160 - 120) \end{array} \right]}{160} \quad (13)$$

314 where θ_i ($i = 5, 10, 20, 40, 60, 80, 120$ and 160 cm) was calculated by taking a
315 weighted average of the measured values in the canopy and bare surface patches,

$$316 \quad \theta_i = M_A \times \theta_{i,c} + (1 - M_A) \times \theta_{i,b} \quad (14)$$

317 where $\theta_{i,c}$ and $\theta_{i,b}$ refer to the measured soil water contents of canopy patch and bare
318 soil patch at the depth of i cm, respectively.

319

320 3.3 Statistical analysis

321 In this study, we chose daily data in Period I to analyze the correlations between
322 E_T and the three controlling factors (E_{TP} , NDVI and f_s). We used several common
323 functions (e.g., an exponential function, a linear function, a logarithmic function and a
324 quadratic function) to fit these correlations. We found that the determination coefficient
325 (R^2) of the linear function was generally the highest. Therefore, in this study, we chose
326 the linear function to fit the correlations between E_T and the three controlling factors.
327 Additionally, significant t -test was performed to evaluate the degrees of these
328 correlations. Moreover, data on rainy days was removed because E_T values were gap-
329 filled rather than measured.

330

331 4 Results

332 4.1 Footprint and energy balance closure

333 Based on the footprint model, we got the half-hourly scatter data (Eq. 2), and
334 according to the wind rose diagram (Fig. 3a), the prevailing wind directions at this site
335 were northwest and southeast. Therefore, we chose an ellipse to enclose the scatters and
336 simulate the footprint (Fig. 3b). Under unstable conditions, 93% of half-hourly flux
337 data plotted within the ellipse.

338 Additionally, we measured the boundary of zone B in October 2013 when the land
339 use/cover condition in zone B had stopped changing (Fig. 3b). There were 11 pixels
340 (250 m × 250 m) in zone A and 19 pixels (250 m × 250 m) in zone B, and thus, when
341 calculating the weight-averaged NDVI ($NDVI_w$) within the footprint, we chose the
342 weighted coefficient as $\beta = 11/(11 + 19)$.

343 [Figure 3 is to be inserted here]

344 EC system performance was assessed by the energy balance closure which was
345 calculated by conducting the linear regression between available energy ($R_n - G$) and
346 the sum of surface fluxes ($\lambda E_T + H$), which is also used to examine the quality of flux
347 data (Wilson et al., 2002). The linear regression yielded a slope of 0.87, an intercept of
348 -1.42 W m^{-2} , and an R^2 of 0.82. These indicators suggested that the measurements at
349 our experimental site provided reliable flux data and that the EC measurements
350 underestimated the sum of the surface fluxes to the extent of 13%. Many researchers
351 have investigated energy imbalance (Barr et al., 2006; Wilson et al., 2002; Franssen et
352 al., 2010), and there is a consensus that it is difficult to examine the exact reasons for
353 the imbalance.

354

355 4.2 Characteristics of environmental variables

356 A brief summary of key environmental variables is presented in this section. Four-
357 year and long-term (1954-2014) average monthly values of D_s , T_a , R_H , and P are
358 shown in Fig. 4. Monthly D_s was much higher than the long-term average monthly
359 values, except in July and September. The highest value of D_s was observed in May
360 (299.5 h) and the lowest was observed in February (206.6 h). The seasonal
361 characteristics of T_a showed a highly similar pattern with that of long-term average
362 monthly values, and the differences were less than 1 °C, except in July, January, and
363 March. The highest value of T_a was observed in July (22.1 °C) and the lowest was
364 observed in December (-8.1 °C). The values of R_H were almost lower than the long-
365 term average monthly values, especially in March and April. The highest R_H was
366 observed in September (65.4%) and the lowest was observed in March (35.1%). The
367 seasonal distributions of P were consistent with the long-term average monthly values,
368 and 89.7% of P occurred in the growing season. P was highest in July (120.5 mm) and
369 lowest in January (0.3 mm).

370 [Figure 4 is to be inserted here]

371 The inter-annual characteristics of daily T_a , D_s , R_H , θ_r , groundwater level
372 (GWL), and total P in the growing season of each period are listed in Tab. 1.

373 [Table 1 is to be inserted here]

374 The values of T_a , R_H , P , and θ_r in the growing season of Period IV were the
375 lowest compared to those in other three periods. Periods I-III were all wet years, while
376 Period IV was a dry year. The values of θ_r in Periods I-III were similar, however, θ_r

377 decreased by $0.0113 \text{ m}^3 \text{ m}^{-3}$ in Period IV. The mean GWL in Period III was the
378 shallowest.

379

380 4.3 Seasonal variations in E_T due to climate variability and vegetation phenology

381 The seasonal curve of E_T in each year had a single peak value (Fig. 5a), with higher
382 E_T appearing mostly in the growing season while lower appeared in the non-growing
383 season. The daily E_T ranged from 0.0 mm day^{-1} to 6.8 mm day^{-1} during the four periods,
384 the highest E_T was observed on 22 June 2013, which was the day after a continuous
385 rainfall event that extended from 19 June 2013 to 21 June 2013 (90.3 mm). The lowest
386 E_T appeared on 28 November 2012, which was in the frozen period (late November to
387 early March at our study site). On rainy days, E_{TP} (Fig. 5b) was low due to low net
388 radiation and air temperature. E_{TP} ranged from 0.2 mm day^{-1} in December 2011 to 17.9
389 mm day^{-1} in September 2013.

390 [Figure 5 is to be inserted here]

391 The seasonal NDVI curve for natural land use/cover condition (in zone A during
392 Periods I-IV and in zone B during Period I) represented the process of natural
393 vegetation phenology and it had a single peak value in each year (Fig. 5c). In early May,
394 the seasonal NDVI curve began to increase as the native vegetation entered the growing
395 season, and a maximum value (0.27 ± 0.01) was reached in July or August. In the winter,
396 the daily NDVI remained relatively constant (0.13 ± 0.01). f_s (Fig. 5d) increased
397 rapidly in response to rainfall events of more than 5 mm a day and decreased rapidly
398 one or two days after rainfall events. From late November to early March, there was a
399 frozen period when the soil water content was below the wilting point. The groundwater

400 level changed obviously in the monsoon season (July to September) and mildly in the
401 winter (December to February).

402 [Figure 6 is to be inserted here]

403 The linear correlations between E_T and the three controlling factors all passed the
404 t -test at a 95% confidence level. The R^2 value of the correlation between E_T and
405 $NDVI_w$ ($NDVI_w = NDVI_A \times \beta + NDVI_B \times (1 - \beta)$) was the largest, indicating that
406 NDVI was highly correlated with the daily variations in E_T . To better quantify the
407 effects of the phenological process on E_T , the correlation between daily f_v and $NDVI_w$
408 in Period I was analyzed (Fig. 7a).

409 [Figure 7 is to be inserted here]

410 A positive linear regression was found between f_v and $NDVI_w$ (Fig. 7a). The
411 slope of the linear regression was used to evaluate the degree of the correlation between
412 f_v and vegetation phenological process. We found that when $NDVI_w$ increased one
413 unit, f_v increased approximately 1.86 units.

414

415 4.4 Inter-annual variations in E_T due to land use/cover change

416 During the four periods, in zone A, the NDVI values of each period were similar
417 because the land use/cover condition did not change. While in zone B, the peak values
418 of NDVI first declined from 0.28 to 0.15 (Period I to Period III) due to the land
419 use/cover condition changed from mixed vegetation to bare soil. The peak NDVI values
420 then increased to 0.22 (Period IV) due to grass recovery (Fig. 5c). An interesting
421 phenomenon was observed accompanied by the changing process of land use/cover

422 conditions: E_T in the growing season gradually increased from Period I to III (Tab. 2),
423 while it increased greatly in Period IV even with less precipitation, because a mass of
424 soil water and ground water was consumed to satisfy the E_T demand (Fig. 5e).

425 [Table 2 is inserted to be here]

426 Compared with Period I, D_{lu} values in Period II and Period III gradually increased,
427 while D_{lu} in Period IV decreased. Taking August in each period as an example, in
428 Period I, D_{lu} was 0.2%, while in Periods II-IV, D_{lu} were 2.9%, 12.6%, and 8.6%,
429 respectively. In order to eliminate the influence of vegetation phenological change on
430 E_T , we chose the growing season of each period to analyze the correlation between f_v
431 and D_{lu} .

432 The quantitative results of the correlation between D_{lu} and f_v are shown in Fig.
433 7b. From Period I to Period III, as land surface characteristics changed (the natural
434 vegetation in zone B was cleared, the fixed and semi-fixed sand dunes were bulldozed,
435 and the BSCs and dry sand layers were disappeared), f_v increased, and this increase
436 was more evident in Period III (from 78.5 to 88.1). When the land use/cover conditions
437 in zone B gradually changed from bare soil to sparse grassland due to the self-restoring
438 capacity of nature, f_v increased significantly (from 88.1 to 111.3).

439

440 5 Discussion

441 5.1 Implications of the effects of phenological change on E_T

442 The correlations between E_T and its controlling factors suggest that at our
443 experimental site, NDVI is the predominant factor that influences the seasonal
444 variations in E_T . The positive linear relationship between f_v and NDVI suggests that

445 transpiration is likely controlled by the stomatal conductance and the numbers of
446 stomata, which are proportional to the leaf area (Pearcy et al., 1989; Turrell, 1947),
447 rather than the atmospheric water demand represented by E_{TP} .

448 Various studies have assessed the correlation between vegetation phenological
449 change and E_T , and these results generally reflected consistent and positive linear
450 relationships (Nouri et al., 2014; Rossato et al., 2005; Duchemin et al., 2006; Glenn et
451 al., 2008). However, for different vegetation species, phenological change has effects
452 on E_T to different degrees. Relative strong regressions between NDVI and E_T have been
453 reported at forested sites (Loukas et al., 2005; Nouri et al., 2014; Chong et al., 2007)
454 and grass-covered sites (Kondoh and Higuchi, 2001; Nouri et al., 2014), with
455 determination coefficients higher than 0.7. These results reflect the strong control
456 between phenological changes and E_T . Thus, we speculate that for high vegetated
457 ecosystems, phenological change may have a significant control on E_T . However, in
458 low vegetated ecosystems such as the sparse shrubland in this study, the relationship
459 between E_T and phenological change is thus positive but relatively weak.

460

461 5.2 Possible reasons for the effects of land use/cover changes

462 During Periods I-IV, the land use/cover conditions at our experimental site
463 underwent changes associated with two processes: land degradation process (Periods
464 II-III) and vegetation rehabilitation process (Period IV). Notable results were observed
465 during these two processes: (1) E_T and normalized E_T values both increased and (2)
466 normalized E_T increased much faster during the vegetation rehabilitation process than

467 it did during the land degradation process.

468 The effect of phenological change on E_T demonstrate that E_T decreases with leaf
469 browning. Thus, we expect that E_T will also decrease if leaves are cleared by human
470 activities. However, during Periods II-III, not only leaves were cleared, but also other
471 land surface properties were changed (all branches were cut, sand dunes (fixed and
472 semi-fixed) were bulldozed, and the dry sand layers and BSCs were destroyed),
473 resulting in complex land use/cover conditions. These altered land surface properties
474 might contribute to the increase in E_T . Previous studies demonstrated that dry sand
475 layers and BSCs could effectively restrict the soil evaporation rate (Wang et al., 2006;
476 Lv et al., 2006; Liu et al., 2006; Chen and Dong, 2001; Yang et al., 2015; Fu et al., 2010;
477 Liu, 2012). However, the bulldozing of sand dunes at our experimental site made the
478 elevation of the flat soil surface lower than the average elevation of the undisturbed soil
479 surface (approximately 1.5 m lower, Fig. 2d), making the groundwater depth was much
480 shallower than the pre-disturbance depth. Thus, the formation of dry sand layers was
481 restricted due to the shallow groundwater level. In this situation with the destroyed
482 BSCs and the disappeared dry sand layers, the sufficient groundwater supply (Li and
483 Li, 2000) accelerated the loss of water that stored in shallow soil through evaporation.
484 The enhanced soil evaporation offset the inhibiting effect of transpiration due to leaves
485 clearing, which made E_T increase.

486 A secondary reason for the increase in soil evaporation was that the soil layer
487 absorbed more solar radiation during the land degradation process. In Period I, the
488 radiation absorbed by the shadowed soil was the solar radiation transmitted into the

489 canopy of shrubs and grass. However, when the natural vegetation was cleared, the
490 leaves and the branches were also removed, which made the shadowed soil exposed
491 and enhanced the radiation absorbed by the soil, thereby increasing soil evaporation
492 (Martens et al., 2000; Panferov et al., 2001). Moreover, the removal of leaves and
493 branches and the disappearance of sand dunes both altered the land surface albedo,
494 which could directly alter the solar radiation absorbed by the land surface (Dirmeyer
495 and Shukla, 1994; Greene et al., 1999), subsequently leading to the change in E_T .

496 Some inconsistent results regarding the E_T dynamics during land degradation
497 process were reported. A portion of studies reported that E_T decreased during the land
498 degradation process for different reasons. For example, Souza and Oyama (2011) and
499 Snyman (2001) demonstrated that E_T decreased during the land degradation process
500 due to decreased transpiration in semiarid regions. Lu et al. (2011) considered that the
501 low soil water content was the main reason for the decrease in E_T during the land
502 degradation process. Mao and Cherkauer (2009) also reported a decrease in E_T when
503 land use/cover condition was converted from forest to grass or cropland in the Great
504 Lakes region. However, contrasting results were also reported regarding the effects of
505 land degradation on E_T . Hoshino et al. (2009) found that there was no difference in E_T
506 during the land degradation process associated with overgrazing in a semiarid
507 Mongolian grassland, and they hypothesized that the reason for this lack of change
508 might be the short grazing time (2 years). Li et al. (2013) demonstrated that the warming
509 air temperature was the main cause of increased E_T during the land degradation process
510 on the Qinghai-Tibet Plateau. Throughout the above studies of E_T during land

511 degradation process, we found it difficult to accurately describe the trends in E_T , even
512 when the land degradation was only manifest by less vegetation coverage. Therefore,
513 at our study site with complex land surface properties (sand dunes, dry sand layers and
514 BSCs), the effect of land degradation on E_T was much more complicated.

515 During the vegetation rehabilitation process (Period IV), f_v increased significantly
516 due to the rehabilitation of grass in zone B, even though less precipitation was observed
517 compared with other periods (Periods I, II and III). The rehabilitation of grass, rather
518 than shrubs, was due to the sufficient groundwater supply, which resulted from
519 bulldozing the sand dunes. Previous researchers reported that sparse shrubs more
520 commonly grew at the top of sand dunes and grass grew at the bottom of sand dunes
521 because the difference between groundwater level and the top of sand dunes was larger
522 than that between groundwater level and the bottom of the sand dunes (Lv et al., 2006;
523 Chen and Dong, 2001). Because transpiration increases with vegetation greening (as
524 demonstrated in section 4.3), the regrowing grass would enhance plant transpiration
525 supplied by the sufficient groundwater. More importantly, the transpiration rate of grass
526 is higher than that of shrubs because shrubs are easier to survive in water-limited
527 conditions (Yang et al., 2014; Wang et al., 2002; Wu, 2006). Therefore, in the vegetation
528 rehabilitation process, the enhancement of transpiration rate in Period IV was much
529 higher than that in Periods I-III. Similar conclusions regarding increased E_T due to the
530 enhanced transpiration during the vegetation rehabilitation process were reported (Qiu
531 et al., 2011; Yang et al., 2014; Sun et al., 2006; Li et al., 2009). Meanwhile, the
532 regrowing grass could reduce the radiation absorbed by the soil and hence reduce soil

533 evaporation. However, the interception of radiation by the grass canopy was expected
534 to be smaller than that by the mixed shrub and grass canopy in Periods I-III because the
535 leaf area index of grass was smaller than the sum of leaf area and stem area indexes of
536 the mix of shrubs and grass. Therefore, the reduction in soil evaporation in Period IV
537 might be small compared with the increase in soil evaporation in Periods I-III.

538 We noticed that the GWL decreased continuously from Period III to Period IV due
539 to the enhanced E_T by the regrowth of grass and relative low precipitation, and the
540 regrowing grass has a higher transpiration rate than that of the native mixed shrub and
541 grass. Therefore, we hypothesize that if the land use/cover condition of zone B
542 continues to be grassland over the next several years, the groundwater level will
543 decrease due to the larger consumption, making the soil water condition gradually
544 become poorer for the growth of grass. Then, in this situation, the grassland is expected
545 to degrade to shrubland in zone B because shrubs are easier to survive in water-limited
546 ecosystems. Furthermore, in the next few years, potatoes will be planted in zone B.
547 However, the water requirement of potato is more than 320 mm in the growing season
548 (Qin et al., 2013; Liu et al., 2010) and the water consumption is more than that of natural
549 grass (Qin et al., 2013, 2014; Hou et al., 2010). Thus, irrigation is necessary for planting
550 potatoes during the growing season in water-limited ecosystems (Fulton et al., 1970;
551 Liu et al., 2010; Fabeiro et al., 2001). Our results imply that the groundwater level might
552 continue to decrease faster with the growth of potatoes in the future, which may lead to
553 a more fragile ecosystem.

554

555 6 Conclusion

556 In this study, seasonal and inter-annual features of E_T were analyzed. Daily E_T was
557 in a range from 0.0 mm day⁻¹ to 6.8 mm day⁻¹ during the four periods. NDVI was the
558 predominant factor that influences the seasonal variations in E_T , and vegetation
559 greening had a positive effect on E_T . During the land degradation process (Periods II-
560 III), when natural vegetation (including leaves and branches), sand dunes, dry sand
561 layers, and BSCs were all bulldozed, E_T increased at a mild rate. During the vegetation
562 rehabilitation process (Period IV) with less precipitation, E_T increased at a faster rate
563 than that in the degradation process. Our study demonstrated that when land use/cover
564 condition changed by human activities, the underlying mechanisms that influence E_T
565 were complex, and vegetation type, topography and soil surface characteristics may all
566 contribute to the changes in E_T . Furthermore, our results suggest that when we simulate
567 the effects of land use/cover change on hydrological processes, vegetation factor might
568 not be the unique factor to parameterize, instead, the integrated effects of land surface
569 and vegetation conditions should be considered. Our study also provides a scientific
570 reference to the regional sustainable management of water resources in the context of
571 intensive agricultural reclamation.

572

573 **Acknowledgements**

574 This research was supported by the National Natural Science Foundation of China
575 (Project No. 91225302), the National Key Research and Development Program of
576 China (2016YFC0402404 and 2016YFC0402406), the Basic Research Fund Program

577 of State key Laboratory of Hydrosience and Engineering (Grant No. 2014-KY-04) and
578 the Basic Research Plan of Natural Science of Shaanxi Province (2016JQ5105). We
579 thank A. W. Jayawardena for language suggestions and constructive comments of the
580 manuscript.

581

582 **References:**

583 Allen, R. G., Pereira, L. S., Raes, D., Smith, M.. Crop evapotranspiration-Guidelines
584 for computing crop water requirements-FAO Irrigation and drainage paper 56. FAO,
585 Rome, 300(9), D05109, 1998.

586 An, H., An, Y.: Soil moisture dynamics and water balance of *Salix psammophila* shrubs
587 in south edge of Mu Us Sandy Land. *Journal of applied ecology* 22, 2247-2252, 2011
588 (in Chinese)

589 Baldocchi, D. D., Wilson K. B.: Modeling CO₂ and water vapor exchange of a
590 temperate broadleaved forest across hourly to decadal time scales, *Ecological*
591 *Modelling*, 142, 155-184, 2001.

592 Barr, A. G., Morgenstern, K., Black, T. A., McCaughey, J. H., Nesic, Z.: Surface energy
593 balance closure by the eddy-covariance method above three boreal forest stands and
594 implications for the measurement of the CO₂ flux. *Agricultural and Forest Meteorology*,
595 140, 322-337, 2006.

596 Chen, S., Chen, J., Lin, G., Zhang, W., Miao, H., Wei, L., ... Han, X.: Energy balance
597 and partition in Inner Mongolia steppe ecosystems with different land use
598 types. *Agricultural and Forest Meteorology*, 149(11), 1800-1809, 2009.

599 Chen, Y., Xia, J. Z., Liang, S. L., Feng, J. M., Fisher, J. B., Li, X., Li, X. L., Liu, S. G.,
600 Ma, Z. G., Miyata, A., Mu, Q. Z., Sun, L., Tang, J. W., Wang, K. C., Wen, J., Xue, Y.
601 J., Yu, G. R., Zha, T. G., Zhang, L., Zhang, Q., Zhao, T. B., Zhao, L. and Yuan, W. P.:
602 Comparison of satellite-based evapotranspiration models over terrestrial ecosystems in
603 China. *Remote Sensing of Environment*, 140, 279-293, 2014.

604 Chong. Lo Seen, D., Mougin, E., Gastellu-Etchegorry, J. P.: Relating the global
605 vegetation index to net primary productivity and actual evapotranspiration over
606 Africa. *Remote Sensing*, 14(8), 1517-1546, 1993.

607 Cornelissen, T., Diekkrüger, B., Giertz, S.: A comparison of hydrological models for
608 assessing the impact of land use and climate change on discharge in a tropical
609 catchment, *Journal of Hydrology*, 498, 221-236, 2013.

610 Dong, X. J., Zhang, X. S.: Some observations of the adaptations of sandy shrubs to the
611 arid environment in the Mu Us Sandland: leaf water relations and anatomic features.
612 *Journal of Arid environments*, 48:41-48, 2001.

613 DeFries, R., Eshleman, K. N.: Land - use change and hydrologic processes: A major
614 focus for the future. *Hydrological processes*, 18(11), 2183-2186, 2004.

615 Ding, R. S., Kang, S. Z., Zhang, Y. Q., Du, T. S.: Multi-layer model of water vapor and
616 heat fluxes over maize field in an arid inland region. *ShuiLiXueBao*, 45(1), 27-35, 2014
617 (in Chinese)

618 Dirmeyer, P. A., & Shukla, J.: Albedo as a modulator of climate response to tropical
619 deforestation. *Journal of Geophysical Research: Atmospheres*, 99 (D10), 20863-20877,
620 1994.

621 Duchemin, B., Hadria, R., Erraki, S., Boulet, G.; Maisongrande, P.; Chehbouni, A.;
622 Escadafal, R., Ezzahar, J.; Hoedjes, J.C.B., Kharrou, M.H.; et al. Monitoring wheat
623 phenology and irrigation in Central Morocco: On the use of relationships between
624 evapotranspiration, crops coefficients, leaf area index and remotely-sensed vegetation
625 indices. *Agric. Water Manag.* 79, 1–27, 2006.

626 Fabeiro, C. M. D. S. O. F., de Santa Olalla, F. M., De Juan, J. A.: Yield and size of
627 deficit irrigated potatoes. *Agricultural Water Management*, 48(3), 255-266, 2001.

628 Falge, E., Baldocchi, D., Olson, R., Anthoni, P., Aubinet, M., Bernhofer, C., Burba, G.,
629 Ceulemans, R., Clement, R., Dolman, H., Granier, A., Gross, P., Grunwald, T.,
630 Hollinger, D., Jensen, N. O., Katul, G., Keronen, P., Kowalski, A., Lai, C. T., Law, B.
631 E., Meyers, T., Moncrieff, H., Moors, E., Munger, J. W., Pilegaard, K., Rannik, U.,
632 Rebmann, C., Suyker, A., Tenhunen, J., Tu, K., Verma, S., Vesala, T., Wilson, K. and
633 Wofsy, S.: Gap filling strategies for long term energy flux data sets. *Agricultural and*
634 *Forest Meteorology*, 107, 71-77, 2001.

635 Falamarzi, Y., Palizdan, N., Huang, Y. F., Lee, T. S.. Estimating evapotranspiration
636 from temperature and wind speed data using artificial and wavelet neural networks
637 (WNNs). *Agricultural Water Management*, 26-36, 2014.

638 Fernández, O. A., Gil, M. E., Distel, R. A.: The challenge of rangeland degradation in
639 a temperate semiarid region of Argentina: the Caldenal. *Land Degradation &*
640 *Development*, 20(4), 431-440, 2009.

641 Feddema, J. J., Freire, S. C.: Soil degradation, global warming and climate impacts,
642 2001.

643 Feng, Q.. Preliminary study on the dry sand layer of sandy land in semi-humid region.
644 Arid zone research, 11,1994 (in Chinese).

645 Fratini, G., Mauder, M.: Towards a consistent eddy-covariance processing: an
646 intercomparison of EddyPro and TK3, Atmospheric measurement techniques, 7, 2273-
647 2281, 2014.

648 Franssen, H. J., Stoeckli, R., Lehner, I., Rotenberg, E. and Seneviratne, S. I.: Energy
649 balance closure of eddy-covariance data: A multisite analysis for European FLUXNET
650 stations. Agricultural and forest meteorology, 150, 1553-1567, 2010.

651 Fernández, R.J.: Do humans create deserts? Trends Ecol. Evol. 17 (1), 6–7, 2002.

652 Fu. G. J., Liao, C. Y., Sun, C. Z.: The effect of soil crust to water movement in
653 maowusu sandland. Journal of northwest forestry university, 25: 7-10, 2010 (in Chinese)

654 Fulton, J. M.: Relationship of root extension to the soil moisture level required for
655 maximum yield of potatoes, tomatoes and corn. Canadian Journal of Soil Science, 50,
656 92-94, 1970.

657 Gao, S., Pan, X., Cui, Q., Hu, Y., Ye, X., Dong, M.: Plant interactions with changes in
658 coverage of biological soil crusts and water regime in Mu Us Sandland, china. PloS
659 one, 9(1), e87713, 2014.

660 Ge, Q., Wang, H., Dai, J.: Phenological response to climate change in China: a meta -
661 analysis. Global change biology, 21(1), 265-274, 2015.

662 Glenn, E.; Huete, A.; Nagler, P.; Nelson, S. Relationship between remotely-sensed
663 vegetation indices, canopy attributes and plant physiological processes: What
664 vegetation indices can and cannot tell us about the landscape. Sensors 2008, 8, 2136–

665 2160.

666 Greene, E.M., Liston, G.E., Pielke, R.A.S.: Relationships between landscape,
667 snowcover depletion, and regional weather and climate. *Hydrological Processes* 13,
668 2453–2466, 1999.

669 Gu, Y., Brown, J. F., Verdin, J. P., Wardlow, B.: A five - year analysis of MODIS
670 NDVI and NDWI for grassland drought assessment over the central Great Plains of the
671 United States. *Geophysical Research Letters*,34(6), 2007.

672 Guo, K., Dong, X. J. and Liu, Z. M.: Characteristics of soil moisture content on sand
673 dunes in mu us sandy grassland: why artemisia ordosica declines on old fixed sand
674 dunes, *Acta phytocologica sinica*, 24, 243-247, 2000 (in Chinese)

675 Gutman, G. and Ignatov, A.: The derivation of the green vegetation fraction from
676 NOAA/AVHRR data for use in numerical weather prediction models, *International*
677 *Journal of Remote Sensing*, 19, 1533-1543, 1998.

678 Hargreaves, G. H., Samani, Z. A.. Reference crop evapotranspiration from
679 temperature. *Applied engineering in agriculture*, 1(2), 96-99, 1985.

680 Hatchett, B., Hogan, M., Grismer, M.: Mechanical mastication thins Lake Tahoe forest
681 with few adverse impacts. *California Agriculture*, 60(2), 77-82, 2006.

682 Hoshino, A., Tamura, K., Fujimaki, H., Asano, M., Ose, K., Higashi, T.: Effects of crop
683 abandonment and grazing exclusion on available soil water and other soil properties in
684 a semi-arid Mongolian grassland. *Soil and tillage research*, 105(2), 228-235, 2009.

685 Hou, X.Y., F.X. Wang, J.J. Han, S.Z. Kang, S.Y. Feng.: Duration of plastic mulch for
686 potato growth under drip irrigation in an arid region of Northwest China. *Agricultural*

687 and Forest Meteorology, 150, 115–121, 2010.

688 Heish, C. I., Katul G. and Chi, T. W.: An approximate analytical model for footprint
689 estimation of scalar fluxes in thermally stratified atmospheric flows. *Advances in Water*
690 *Resources*, 23, 765-772, 2000.

691 Hu, H. H., Dai, M. Q., Yao, J. L., Xiao, B. Z., Li, X. H., Zhang, Q. F. and Xiong, L. Z.:
692 Overexpressing a NAM, ATAF, and CUC (NAC) transcription factor enhances drought
693 resistance and salt tolerance in rice, *Proceedings of the National Academy of Sciences*,
694 103, 12987-12992, 2006.

695 Huete, A., Didan, K., Miura, T., Rodriguez, E. P., Gao, X. and Ferreira, L. G.: Overview
696 of the radiometric and biophysical performance of the MODIS vegetation indices.
697 *Remote sensing of environment*, 83, 195-213, 2002.

698 Jarvis, P. G., Mansfield, T. A.. *Stomatal physiology*. 1981.

699 Jarvis P G, McNaughton K G. Stomatal control of transpiration: scaling up from leaf to
700 region[J]. *Advances in ecological research*, 15, 1-49, 1986.

701 Jordan, D., Zitzer, S. F., Hendrey, G. R., Lewin, K. F., Nagy, J., Nowak, R. S., ...
702 Seemann, J. R.: Biotic, abiotic and performance aspects of the Nevada Desert Free -
703 Air CO2 Enrichment (FACE) Facility. *Global Change Biology*, 5(6), 659-668, 1999.

704 Kalvelage, T., Willems, J.: Supporting users through integrated retrieval, processing,
705 and distribution systems at the Land Processes Distributed Active Archive Center, *Acta*
706 *astronautica*, 56, 681-687, 2005.

707 Kim, W., Kanae, S., Agata, Y., Oki, T.: Simulation of potential impacts of land
708 use/cover changes on surface water fluxes in the Chaophraya river basin, Thailand,

709 Journal of Geophysical Research: Atmospheres (1984-2012), 110, 2005.

710 Kondoh, A., Higuchi, A.: Relationship between satellite - derived spectral brightness
711 and evapotranspiration from a grassland. Hydrological processes, 15(10), 1761-1770,
712 2001

713 Lei, Z. D., Yang, S. X. and Xie, S. C.: Soil water dynamics, Tsing-Hua University Press,
714 Beijing, 1988 (in Chinese).

715 Lettermaier, D. P. and Famiglietti, J. S.: Water from on high. Nature, 2006, 444, 562-
716 563.

717 Liang, L., Lu, S. H. and Shang, L. Y.: Numerical simulation of effect of Loess Plateau
718 vegetation change on local climate, Plateau Meteorol, 27, 293-300, 2008.

719 Leuning, R., Kelliher, F. M., Pury, D. D., SCHULZE, E. D.: Leaf nitrogen,
720 photosynthesis, conductance and transpiration: scaling from leaves to canopies. Plant,
721 Cell & Environment, 18(10), 1183-1200, 1995.

722 Li, P. F., Li, B. G.: Study on some characteristics of evaporation of sand dune and
723 evapotranspiration of grassland in Mu Us desert. 3:23-28, 2000 (in Chinese).

724 Li, Z., Liu, W. Z., Zhang, X. C. and Zheng, F. L.: Impacts of land use change and
725 climate variability on hydrology in an agricultural catchment on the Loess Plateau of
726 China, Journal of hydrology, 377, 35-42, 2009.

727 Li, X. L., Gao, J., Brierley, G., Qiao, Y. M., Zhang, J., Yang, Y. W.: Rangeland
728 degradation on the Qinghai - Tibet plateau: Implications for rehabilitation. Land
729 Degradation & Development, 24(1), 72-80, 2013.

730 Li, S., Kang, S., Zhang, L., Du, T., Tong, L., Ding, R., ... Xiao, H.: Ecosystem water

731 use efficiency for a sparse vineyard in arid northwest China. *Agricultural Water*
732 *Management*, 148, 24-33, 2015.

733 Liu, C., Zhang, X., Zhang, Y.: Determination of daily evaporation and
734 evapotranspiration of winter wheat and maize by large-scale weighing lysimeter and
735 micro-lysimeter. *Agricultural and Forest Meteorology*, 111(2), 109-120, 2002.

736 Liu, F.: Point pattern of *Artemisia ordosica* and the impact to soil crust thickness in Mu
737 Us Sandland. Mater Thesis of Beijing Forestry University, 2012 (in Chinese)

738 Liu, X. P., Zhang, T. H., Zhao, H. L., He, Y. H., Yun, J. Y., Li, Y. Q.: Influences of dry
739 sand bed thickness on soil moisture evaporation in mobile dune. *Arid land geography*,
740 29, 2006 (in Chinese)

741 Liu, J. S., Gao, Q., Guo, K., Liu, X. P., Shao, Z. Y., Zhang, Z. C.: Actual evaporation
742 of bare sand dunes in maowusu, china and its response to precipitation pattern. *Journal*
743 *of plant ecology*, 2008, 123-132, 2008

744 Liu, Z. D., Xiao, J. F., Yu, X. Q.: Effects of different soil moisture treatments on
745 morphological index, water consumption and yield of potatoes. *China Rural Water and*
746 *Hydropower*, 8, 1-7, 2010.

747 Loukas, A., Vasiliades, L., Domenikiotis, C. and Dalezios, N. R.: Basin-wide actual
748 evapotranspiration estimation using NOAA/AVHRR satellite data, *Physics and*
749 *Chemistry of the Earth*, 30, 69-79, 2005.

750 Lorup, J. K., Refsgaard, J. C., Mazvimavi, D.: Assessing the effect of land use change
751 on catchment runoff by combined use of statistical tests and hydrological modelling:
752 case studies from Zimbabwe. *Journal of hydrology*, 205(3), 147-163, 1998.

753 Lu, N., Chen, S., Wilske, B., Sun, G., Chen, J.: Evapotranspiration and soil water
754 relationships in a range of disturbed and undisturbed ecosystems in the semi-arid Inner
755 Mongolia, China. *Journal of Plant Ecology*,4(1-2), 49-60, 2011.

756 Lunetta, R.S., Knight, J. F., Ediriwickrema, J., Lyon, J. G., Worthy, L. D.: Land-cover
757 change detection using multi-temporal MODIS NDVI data, *Remote sensing of*
758 *environment*, 105, 142-154, 2006.

759 Lv, Y. Z., Hu, K. L., Li, B. G.: The spatio-temporal variability of soil water in sand
760 dunes in maowusu desert. 43, 2006 (in Chinese).

761 Mackay, D. S., Ewers, B. E., Cook, B. D., Davis, K. J.: Environmental drivers of
762 evapotranspiration in s shrub wetland and an upland forest in northern Wisconsin.
763 *Water resources research*, 43, doi:10.1029/2006WR005149, 2007.

764 Maayar, M., & Chen, J. M.: Spatial scaling of evapotranspiration as affected by
765 heterogeneities in vegetation, topography, and soil texture.*Remote Sensing of*
766 *Environment*, 102(1), 33-51, 2006.

767 Maidment, D. R.: *Handbook of hydrology*, 1992.

768 Mao, D., Cherkauer, K. A.: Impacts of land-use change on hydrologic responses in the
769 Great Lakes region. *Journal of Hydrology*, 374(1), 71-82, 2009.

770 Mauder, M., Liebenthal, C., Göckede, M., Leps, J. P., Beyrich, F., Foken, T.. Processing
771 and quality control of flux data during LITFASS-2003.*Boundary-Layer*
772 *Meteorology*, 121(1), 67-88, 2006. Mo, X. G., Liu, S. X., Lin, Z. H. and Chen, D.:
773 Simulating the water balance of the wuding river basin in the Loess Plateau with a
774 distributed eco-hydrological model, *Acta Geographica Sinica*, 59, 341-347, 2004 (in

775 Chinese)

776 Martens, S. N., D. D. Breshears, and C. W. Meyer.: Spatial distributions of understory
777 light along the grassland/forest continuum: effects of cover, height, and spatial pattern
778 of tree canopies. *Ecological Modeling* 126:79–93, 2000.

779 Nouri, H., Beecham, S., Anderson, S., Nagler, P.: High spatial resolution WorldView-2
780 imagery for mapping NDVI and its relationship to temporal urban landscape
781 evapotranspiration factors. *Remote sensing*, 6(1), 580-602, 2014.

782 Ostwald, M., Chen, D.: Land-use change: Impacts of climate variations and policies
783 among small-scale farmers in the Loess Plateau, China. *Land Use Policy*, 23(4), 361-
784 371, 2006.

785 Pearcy, R. W., Schulze, E. D., Zimmermann, R.: Measurement of transpiration and leaf
786 conductance. *Plant physiological ecology*. Springer Netherlands, 137-160, 1989.

787 Penman, H. L.: National evaporation from open water, bare soil and grass. *Proc. R. Soc.*
788 *London*, A193, 120-145, 1948.

789 Penman, H. L.: *Vegetation and hydrology*, Tech. Comm. 53, Commonwealth Bureau
790 of Soils, Harpenden, England, 1963.

791 Piao, S., Fang, J., Zhou, L., Ciais, P., Zhu, B.: Variations in satellite-derived phenology
792 in China's temperate vegetation. *Global Change Biol.* 12, 672–685, 2006.

793 Papale, D., Reichstein, M., Aubinet, M., Canfora, E., Bernhofer, C., Kutsch, W.,
794 Longdoz, B., Rambal, S., Valentini, R., Vesala, T. and Yakir, D.: Towards a
795 standardized processing of Net Ecosystem Exchange measured with eddy covariance
796 technique: algorithms and uncertainty estimation, 2006.

797 Panferov, O., Knyazikhin, Y., Myneni, R. B., Szarzynski, J., Engwald, S., Schnitzler, K.
798 G., & Gravenhorst, G.: The role of canopy structure in the spectral variation of
799 transmission and absorption of solar radiation in vegetation canopies. IEEE
800 Transactions on Geoscience and Remote Sensing, 39, 2, 241-253, 2001.

801 Qin, S.H., L.L. Li, D. Wang, J.L. Zhang, Y.L. Pu.: Effects of limited supplemental
802 irrigation with catchment rainfall on rain-fed potato in semi-arid areas on the Western
803 Loess Plateau, China. American Journal of Potato Research, 90, pp. 33–42, 2013.

804 Qin, S., Zhang, J., Dai, H., Wang, D., Li, D.: Effect of ridge–furrow and plastic-
805 mulching planting patterns on yield formation and water movement of potato in a semi-
806 arid area. Agricultural Water Management, 131, 87-94, 2014.

807 Qiu, G. Y., Xie, F., Feng, Y. C., Tian, F.: Experimental studies on the effects of the
808 “Conversion of Cropland to Grassland Program” on the water budget and
809 evapotranspiration in a semi-arid steppe in Inner Mongolia, China. Journal of
810 Hydrology, 411(1), 120-129, 2011.

811 Rossato, L.; Alvala, R.C.S.; Ferreira, N.J.; Tomasella, J.: Evapotranspiration estimation
812 in the Brazil using NDVI data. Proc. SPIE 2005, 5976, 377–385.

813 Snyman, H. A.: Water-use efficiency and infiltration under different rangeland
814 conditions and cultivation in a semi-arid climate of South Africa. In Proceedings of the
815 XIX International Grassland Congress, Sao Paulo, Brazil (pp. 965-966), 2001.

816 Souza, D. C., Oyama, M. D.: Climatic consequences of gradual desertification in the
817 semi-arid area of Northeast Brazil. Theoretical and Applied Climatology, 103(3-4),
818 345-357, 2011.

819 Sun, G., Zhou, G., Zhang, Z., Wei, X., McNulty, S. G., Vose, J. M.: Potential water
820 yield reduction due to forestation across China. *Journal of Hydrology*, 328(3), 548-558,
821 2006.

822 Tian, H., Cao, C., Chen, W., Bao, S., Yang, B., Myneni, R. B.: Response of vegetation
823 activity dynamic to climatic change and ecological restoration programs in Inner
824 Mongolia from 2000 to 2012. *Ecological Engineering*, 82, 276-289, 2015.

825 Tong, X., Zhang, J., Meng, P., Li, J., Zheng, N.: Environmental controls of
826 evapotranspiration in a mixed plantation in North China. *International Journal of*
827 *Biometeorology*, 1-12, 2016.

828 Twine, T. E., Kucharik, C. J., Foley, J. A.: Effects of land cover change on the energy
829 and water balance of the Mississippi River basin. *Journal of Hydrometeorology*, 5(4),
830 640-655, 2004.

831 Tucker, C. J.: Red and photographic infrared linear combinations for monitoring
832 vegetation, *Remote Sens. Environ.*, 8, 127-150, 1979.

833 Turrell, F. M.: Citrus leaf stomata: structure, composition, and pore size in relation to
834 penetration of liquids. *The University of Chicago Press* 108, 476-483, 1947.

835 Valipour, M.: Study of different climatic conditions to assess the role of solar radiation
836 in reference crop evapotranspiration equations. *Archives of Agronomy and Soil*
837 *Science*, 61(5), 679-694, 2015.

838 Vanacker, V., Vanderschaeghe, M., Govers, G., Willems, E., Poesen, J., Deckers, J., De
839 Bievre, B.: Linking hydrological, infinite slope stability and land-use change models
840 through GIS for assessing the impact of deforestation on slope stability in high Andean

841 watersheds. *Geomorphology*, 52(3), 299-315, 2003.

842 Vetter, S. H., Schaffrath, D., Bernhofer, C.: Spatial simulation of evapotranspiration of
843 semi-arid Inner Mongolian grassland based on MODIS and eddy covariance
844 data. *Environmental Earth Sciences*, 65(5), 1567-1574, 2012.

845 Wang, M. Y., Guan, S. H., Wang, Y.: Soil moisture regime and application for plants
846 in Maowusu Transition Zone from sandland to desert. 16 (2): 37-44, 2002.

847 Wang, Z., Wang, L., Liu, L. Y., Zheng, Q. H.: Preliminary study on soil moisture
848 content in dried layer of sand dunes in the Mu Us sandland, 26, 2006 (in Chinese).

849 Wang, L., Wang, Q. J., Wei, S. P., Shao, M. A. and Yi, L.: Soil desiccation for Loess
850 soils on natural and regrown areas, *Forest Ecology and Management*, 255, 2467-2477,
851 2008.

852 Wang, L., Wang Z., Liu, L.Y. and Hasi, E.: Field investigation on salix psammophila
853 plant morphology and airflow structure, *Front. For. China*, 2, 136-141, 2006.

854 Wang, S., Wilkes, A., Zhang, Z., Chang, X., Lang, R., Wang, Y., Niu, H.: Management
855 and land use change effects on soil carbon in northern China's grasslands: a
856 synthesis. *Agriculture, Ecosystems & Environment*, 142(3), 329-340, 2011.

857 Wang, Y. Q., Shao, M. A., Zhu, Y. J. and Liu, Z. P.: Impacts of land use and plant
858 characteristics on dried soil layers in different climatic regions on the Loess Plateau of
859 China, *Agricultural and Forest Meteorology*, 151, 437-448, 2011.

860 Wever, L. A., Flanagan, L. B., Carlson, P. J.. Seasonal and interannual variation in
861 evapotranspiration, energy balance and surface conductance in a northern temperate
862 grassland. *Agricultural and Forest Meteorology*, 112(1), 31-49, 2002.

863 Wilson, K., Goldstein, A., Falge, E., Aubinet, M., Baldocchi, D., Berbigier, P.,
864 Bernhofer, C., Ceulemans, R., Dolman, H., Field, C., Grelle, A., Ibrom, A., Law, B. E.,
865 Kowalski, A., Meyers, T., Moncrieff, J., Monson, R., Oechel, W., Tenhunen, J.,
866 Valentini, R. and Verma, S.: Energy balance closure at FLUXNET sites, *Agricultural*
867 *and Forest Meteorology*, 113, 223-243, 2002.

868 Wu, G. X.: Roots' distribution characteristics and fine root dynamics of *Sabina vulgaris*
869 and *Artemisia ordosica* in Mu Us Sandland. Master thesis of Inner Mongolia
870 Agricultural University, 2006.

871 Wu, B., Ci, L. J.: Landscape change and desertification development in the Mu Us
872 Sandland, Northern China. *Journal of Arid Environments*, 50(3), 429-444, 2002.

873 Xiao, C.W., Zhou, G. S., Zhang, X. S., Zhao, J. Z. and Wu, G.: Responses of dominant
874 desert species *Artemisia ordosica* and *Salix psammophila* to water stress,
875 *Photosynthetica*, 43, 467-471, 2005.

876 Yang, Y. M., Yang, G. H., Feng, Y. Z.: Climatic variation and its effect on
877 desertification in 45 recent years in Mu Us sandland. 35 (12): 87-92, 2007.

878 Yang, Y., Bu, C., Mu, X., Zhang, K.: Effects of differing coverage of moss - dominated
879 soil crusts on hydrological processes and implications for disturbance in the Mu Us
880 Sandland, China. *Hydrological Processes*, 29(14), 3112-3123, 2015.

881 Yang, L., Wei, W., Chen, L., Chen, W., Wang, J.: Response of temporal variation of soil
882 moisture to vegetation restoration in semi-arid Loess Plateau, China. *Catena*, 115, 123-
883 133, 2014.

884 Yuan, P. F., Ding, G. D., Wang, W. W., Wang, X. Y., Shi, H. S.: Characteristics of

885 rainwater infiltration and evaporation in Mu Us Sandland. *Science of Soil and Water*
886 *Conservation*, 4, 004, 2008.

887 Zeng, N., Yoon, J.: Expansion of the world's deserts due to vegetation - albedo
888 feedback under global warming. *Geophysical Research Letters*, 36(17), 2009.

889 Zeng B, Yang T-B.: Impacts of climate warming on vegetation in Qaidam area from
890 1990 to 2003. *Environmental Monitoring and Assessment*, 144: 403–417, 2008.

891 Zeng, X. B., and Coauthors.: Coupling of the common land model to the NCAR
892 community climate model. *J. Climate*, 15, 1832–1854, 2002.

893 Zhang, Y., Munkhtseteg, E., Kadota, T. and Ohata, T.: An observational study of
894 ecohydrology of a sparse grassland at the edge of the Eurasian cryosphere in Mongolia,
895 *Journal of Geophysical Research: Atmospheres* (1984-2012), 110,
896 doi:10.1029/2004JD005474, 2005.

897 Zhang, Z. P.: Vegetation pattern changes in Mu Us desert and the analysis of water
898 income and expenses: a case study in Mu Us county. Master thesis of Inner Mongolia
899 University, 2006.

900 Zhang, Z. P.: Vegetation pattern changes in Mu Us desert and the analysis of water
901 income and expenses: a case study in wushen county. Mater thesis of Inner Mongolia
902 University, 2006 (in Chinese)

903 Zhang, Z. S., Wang, X. P., Li, X. R., Zhang, J. G.: Soil evaporation in artificially
904 revegetated desert area. *Journal of desert research*, 25, 243-248, 2005 (in Chinese)

905 Zhang, Y. Y., Zhou, Z. F., Cheng, J. H., Dang, H. Z., Li, W.: Soil moisture characteristics
906 of several types of shrubs in different anchored dune positions in maowusu sandy land.

907 42, 73-78, 2010 (in Chinese).

908 Zhang, Q., Manzoni, S., Katul, G., Porporato, A., Yang, D.. The hysteretic

909 evapotranspiration—Vapor pressure deficit relation. *Journal of Geophysical Research:*

910 *Biogeosciences*, 119(2), 125-140, 2014.

911

912 **Figure and table captions**

913 Fig. 1. Location of the Loess Plateau and map of study site (LP: the Loess Plateau;
914 black triangle: flux tower; white triangle: Yulin meteorological station; ①: Tu River;
915 ②: Yuxi River; ③: Yellow River)

916

917 Fig. 2. Land use/cover conditions at the study site: (a) the natural land use/cover
918 condition of shrubland (photo was taken on 6 August 2011); (b) the natural land
919 use/cover condition of grassland (photo was taken on 7 September 2011); (c) the
920 undisturbed zone (natural vegetation) and the disturbed zone (bare soil) in the land
921 degradation process (photo was taken on 26 April 2013); (d) the undisturbed zone
922 (natural vegetation) and the disturbed zone (grassland) during the vegetation
923 rehabilitation process (photo was taken on 16 August 2014)

924

925 Fig. 3. Diagrams of wind rose and footprint: (a) wind rose of the study site by using
926 half-hourly wind speed and wind direction data and (b) simulated footprint by ellipse
927 (the long axis is 1682 m, and the short axis is 1263 m; zone A is the source area in
928 which land use/cover condition did not change, while zone B is the source area in which
929 land use/cover condition did change due to human activities; the white triangle is the
930 flux tower)

931

932 Fig. 4. Seasonal characteristics of four-year and long-term (1954-2014, from Yulin
933 meteorological station) average monthly values of: (a) sunshine duration (D_S); (b) air
934 temperature (T_a); (c) relative humidity (R_H) and (d) total precipitation (P)

935

936 Fig. 5. Seasonal and inter-annual characteristics of daily (a) evapotranspiration (E_T ,
937 mm); (b) potential evapotranspiration (E_{TP} , mm); (c) NDVI in zone A and zone B within
938 the footprint; (d) the soil water stress of the root zone (f_s) and (e) the groundwater level
939 (GWL, m) from 1 July 2011 to 30 June 2015

940

941 Fig. 6. The correlations between daily evapotranspiration (E_T , mm) and its controlling
942 factors: (a) daily potential evapotranspiration (E_{TP} , mm); (b) daily weight-averaged
943 NDVI ($NDVI_w$) within the footprint; (c) daily soil water stress of the root zone (f_s) in
944 Period I by excluding the data on rainy days (r: Pearson's correlation coefficient; T: t-
945 test significance)

946

947 Fig. 7. Quantitative analysis of the correlations between (a) vegetation phenological
948 change ($NDVI_w$) and daily normalized E_T ($f_v = E_T / (E_{TP} \times f_s)$) in Period I (excluded
949 the data on rainy days and frozen days) and (b) the indicator of land use/cover change
950 (D_{lu}) and total normalized E_T ($f_v = E_T / (E_{TP} \times f_s)$) in the growing season of each
951 period.

952

953 Table 1. Daily air temperature (T_a , °C), relatively humidity (R_H , %), total sunshine
954 duration (D_S , h), soil water content of the root zone (θ_r , $m^3 m^{-3}$), the groundwater level
955 (GWL, m), and total precipitation (P , mm) in 1954-2014 and in the growing season of
956 each period (because there were some missing data in Period IV (from 12 September

957 2014 to 23 November 2014 and from 13 March 2015 to 22 April 2015), we excluded
 958 data in these two time ranges of Periods I-III and 1954-2014)
 959

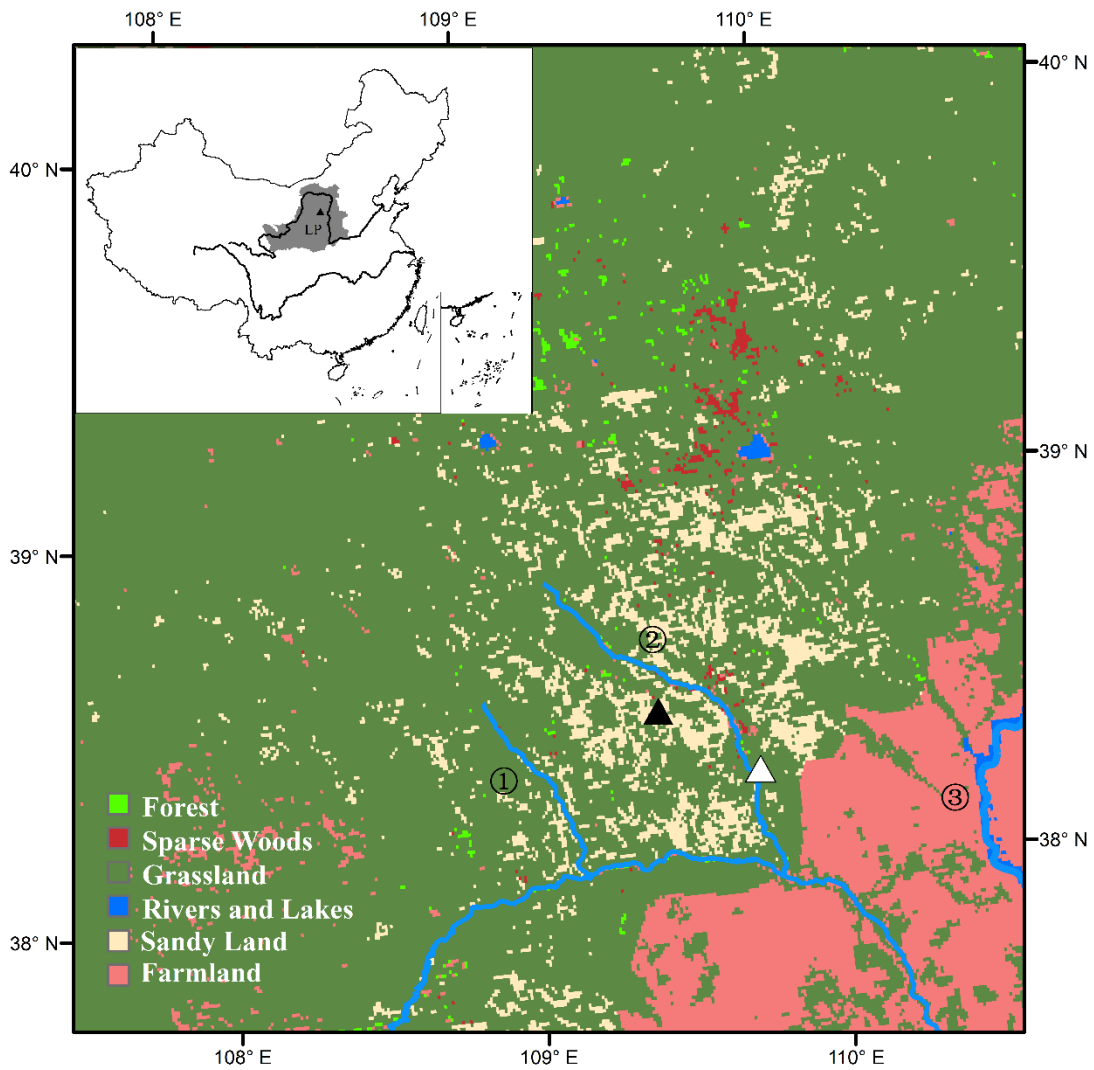
Variable	1954-2014	I	II	III	IV
T_a (°C)	19.8	19.6	20.4	19.9	19.3
R_H (%)	57.7	57.3	54.9	53.4	52
D_S (h)	213.3	220.7	215.8	218.2	220.7
P (mm)	329.8	357.1	384.1	330.2	199.8
θ_r (m ³ m ⁻³)	–	0.077	0.077	0.076	0.064
GWL (m)	–	-3.8	-3.6	-3.0	-3.5

960
 961 Table 2. Typical values of total evapotranspiration (E_T , mm), total potential
 962 evapotranspiration (E_{TP} , mm), the indicator of land use/cover change (D_{lu}), the soil
 963 water stress of the root zone (f_s), and normalized E_T (f_v ($= E_T / (E_{TP} \times f_s)$)) in the
 964 growing season of each period (because there were some missing data in Period IV
 965 (from 12 September 2014 to 23 November 2014 and from 13 March 2015 to 22 April
 966 2015), we removed the values of E_T , E_{TP} and f_s in these two time ranges of Periods I-
 967 III).
 968

	Period	E_T (mm)	E_{TP} (mm)	D_{lu} (%)	f_s (dimensionless)	f_v (dimensionless)
Growing season	I	238.4	876.1	-0.2	0.62	78.1
	II	236.5	870.7	4.6	0.63	79.9
	III	292.1	956	10.4	0.59	86.3
	IV	332.2	937	6	0.37	111.9

970

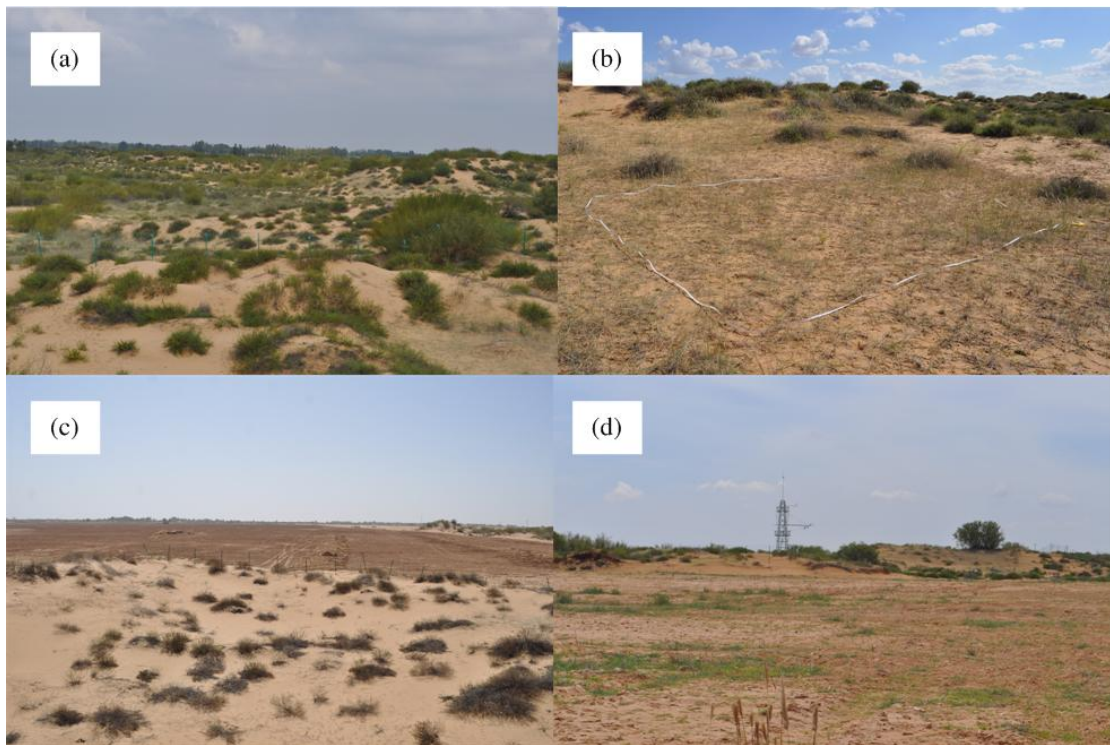
971 Fig. 1



972

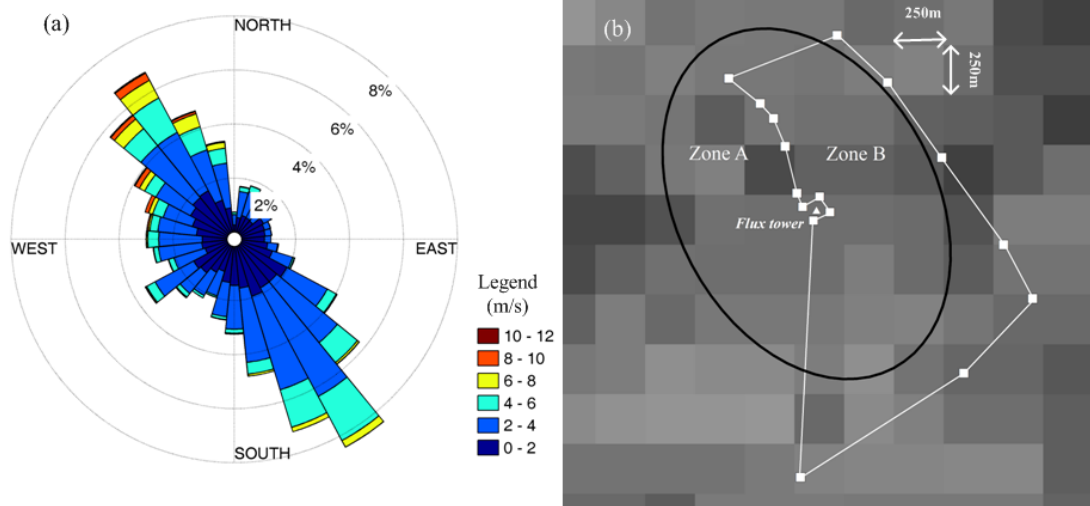
973

974 Fig. 2



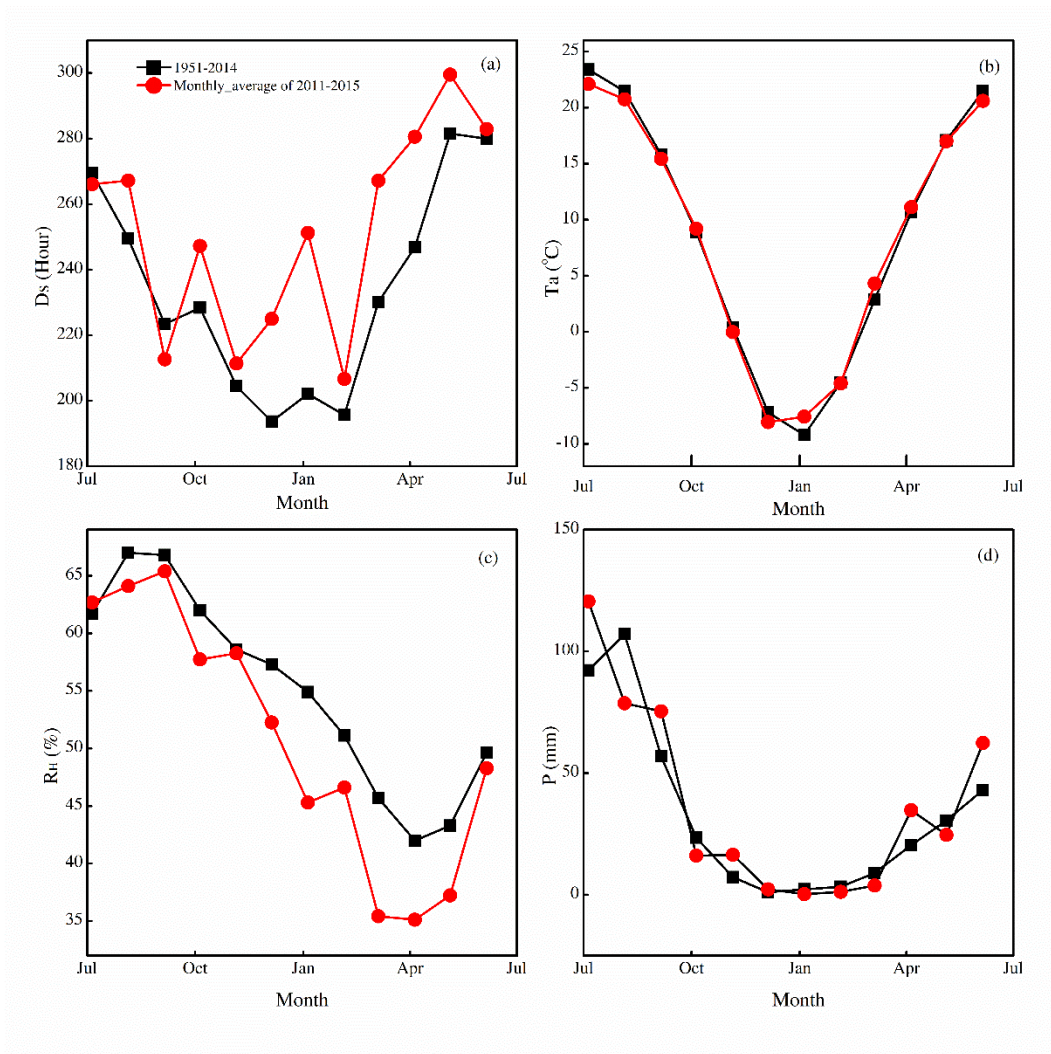
975
976
977
978

979 Fig. 3



980
981
982
983

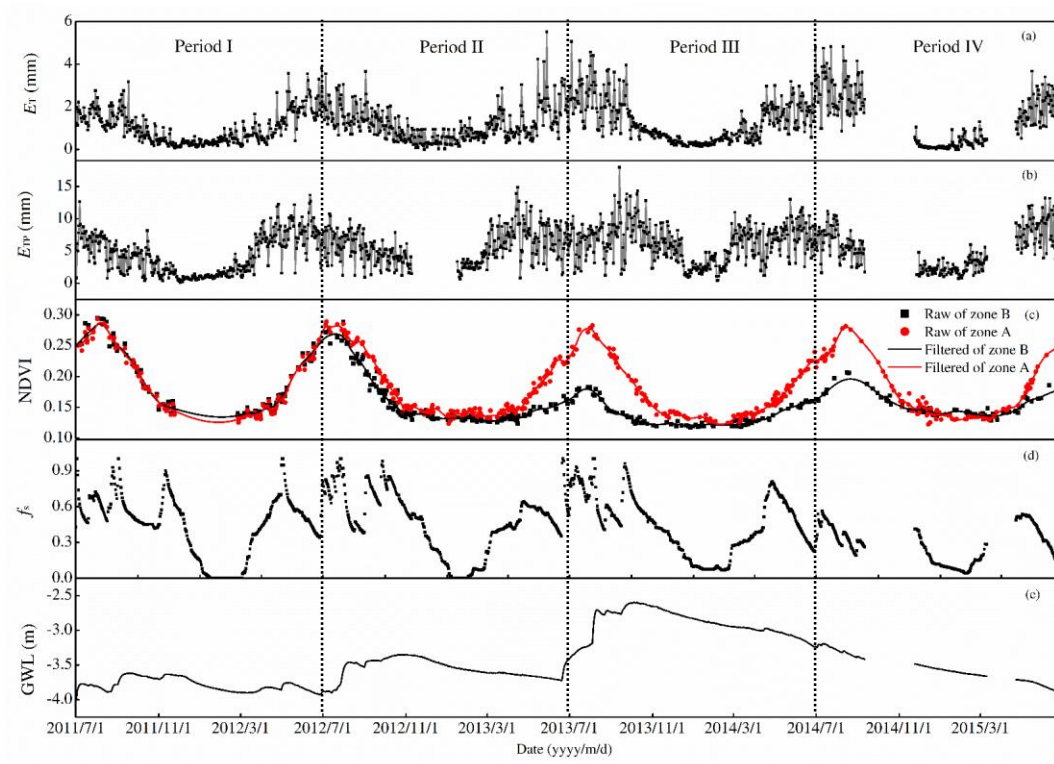
984 Fig. 4



985

986

987 Fig. 5



988

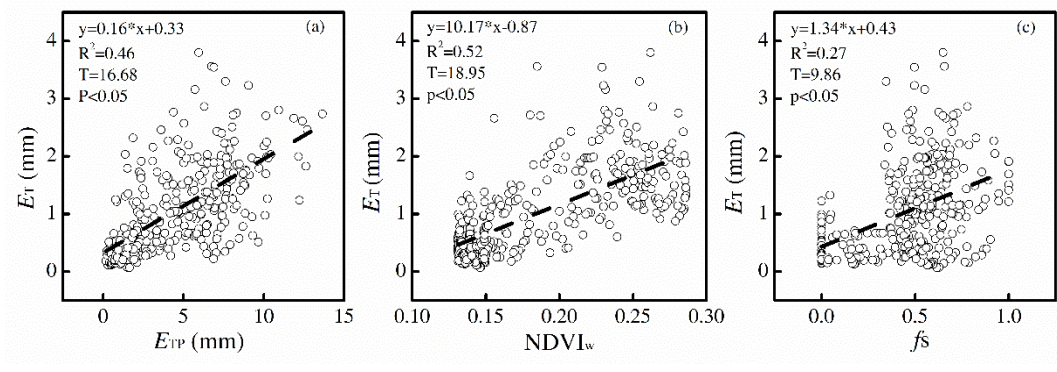
989

990

991

992 Fig. 6

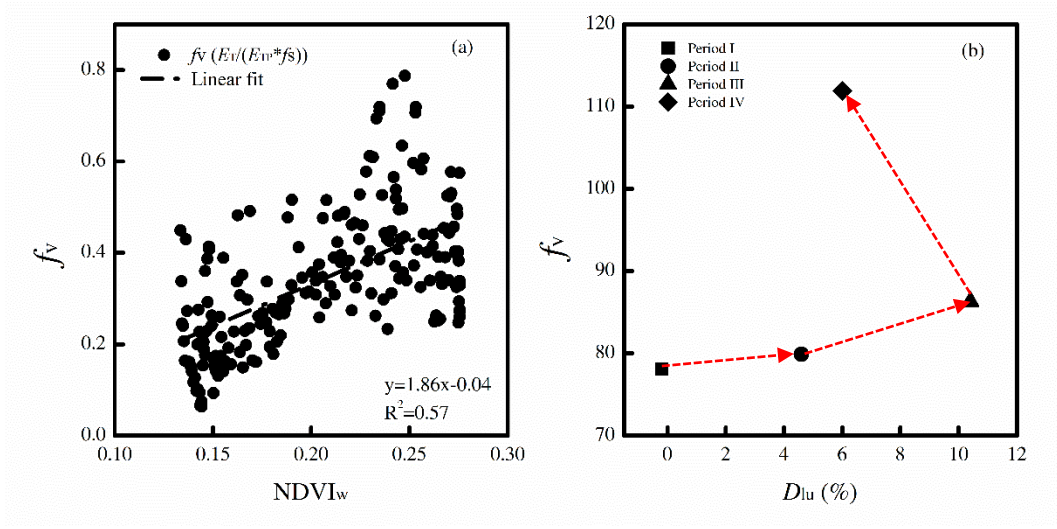
993



994

995

Fig. 7



996

997

998

999

1000

1001